



Washington, D.C.  
March 27-31, 2011

### Paper A-4-03

## NUMERICAL ANALYSIS OF THE RESPONSE OF ADJACENT PIPELINES DURING STATIC PIPE BURSTING

Kazi Rahman<sup>1</sup>, Ian Moore<sup>2</sup>, Richard Brachman<sup>3</sup>

<sup>1</sup> Graduate Student, Department of Civil Engineering, Queen's University, Kingston, ON

<sup>2</sup> Professor, GeoEngineering Centre at Queen's - RMC, Queen's University, Kingston, ON

<sup>3</sup> Associate Professor, GeoEngineering Centre at Queen's - RMC, Queen's University, Kingston, ON

**ABSTRACT:** The expansion of the soil around the pipe being replaced during static pipe bursting causes ground disturbance, and surrounding infrastructure like pipelines are potentially vulnerable. Three-dimensional finite element analyses are being used to investigate the mechanics of soil interacting with other pipes. The progression of a burst head (or expander) through an existing pipeline is simulated using ABAQUS, and the effect of the resulting ground movements on adjacent pipes is calculated. The analysis is evaluated against surface movements observed in a static pipe bursting experiment conducted in a 2 m long, 2 m wide, and 1.6 m deep test cell. Calculated deformations are within 10% of measured values.

The analysis is then used to examine the effect of pipe bursting on both PVC and cast iron water pipes located in the vicinity of the gravity flow pipe being replaced. Firstly, a 122 mm OD (outside diameter) and 7 mm thick PVC pipe is studied, with orientation transverse to the bursting direction, and located 300 mm above the crown of the clay pipe being replaced. The three-dimensional deformations, strains, and stresses in the adjacent PVC pipe are calculated during the progression of the burst head through the clay pipe. Analysis is then conducted to examine the same PVC pipe oriented parallel to the existing clay pipe. Maximum longitudinal PVC pipe strain of about 0.2 % was calculated for both these cases. Next, the analysis is used to examine the impact of bursting on cast iron pipes located transverse and parallel to the pipe being replaced. Both thick ( $D/t = 11.2$ ) and thin ( $D/t = 31.5$ ) pipes are analyzed and the maximum incremental longitudinal strain calculated is 0.04%. This may be sufficient to cause fracture, since it is in addition to strains from thermal and fluid loads, and is more than half of the expected fracture strain (minimum of 0.07% for cast iron water mains examined in Toronto).

### 1. INTRODUCTION

Static pipe bursting is a well known trenchless technology where an existing buried pipe is broken by a metallic expander (burst head), the resulting fragments of the old pipe are pushed outward, and a replacement pipe is pulled through the expanded cavity. Three dimensional ground disturbance results from the expansion of the soil around the old pipe, which can cause serious damage to other infrastructure like adjacent pipelines, Rogers and Chapman (1995), Atalah et al. (1997). Of particular concern during sewer replacement using pipe bursting is disturbance to water and gas pressure pipes lying overhead (Figure 1), since they may be located within the zone of soil uplift. It is therefore desirable to quantify the impact of pipe bursting on these overlying pressure pipelines. Three dimensional

finite element analysis has the potential to calculate the strains, stresses, and deformations of surrounding infrastructure during pipe bursting. This paper introduces that analysis.

The credibility and authority of numerical analyses benefits when calculations are supported by physical measurements. A laboratory test conducted at Queen's University to measure ground deformations during static pipe bursting has been reported by Lapos et al. (2004) and Lapos (2004). A clay pipe with inside diameter (ID) of 146 mm was placed in the 2 m wide by 2 m long by 1.6 m deep test cell developed by Brachman et al. (2001) filled with poorly graded sand (Figure 2). The clay pipe was replaced with an HDPE pipe of 145 mm ID using static pipe bursting. The surface deformations were monitored using surveying prisms placed on the ground surface (Figure 3). The 3D finite element model is evaluated using measurements of surface movement obtained from this experiment.

The analysis is then used to calculate the response of pressure pipes oriented transverse to, and parallel to the axis of the sewer being replaced. The responses of both PVC and Cast Iron (CI) pipes are considered, and the resulting strains are compared to strain limits for these products.

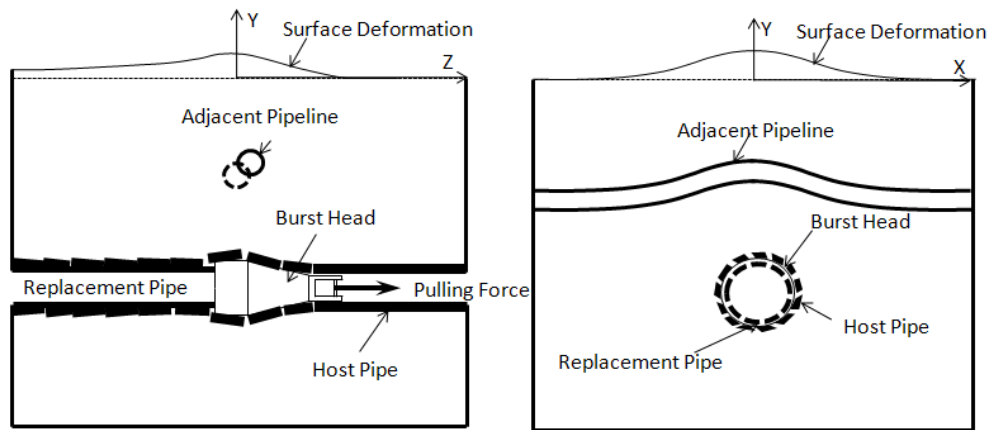


Figure 1. Schematic view of the impact of pipe bursting on adjacent pipeline

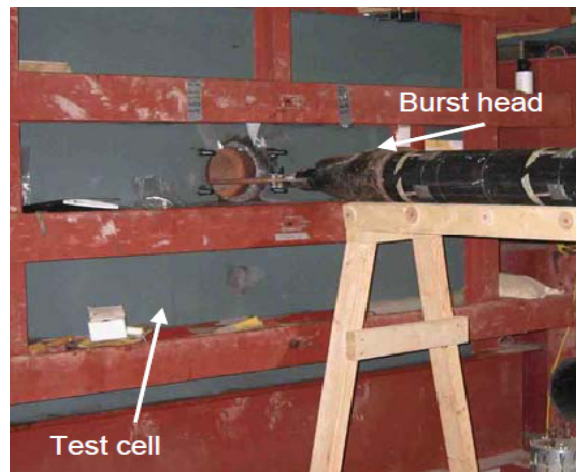


Figure 2. The test cell, burst head and replacement pipe of the laboratory test (Lapos, 2004)

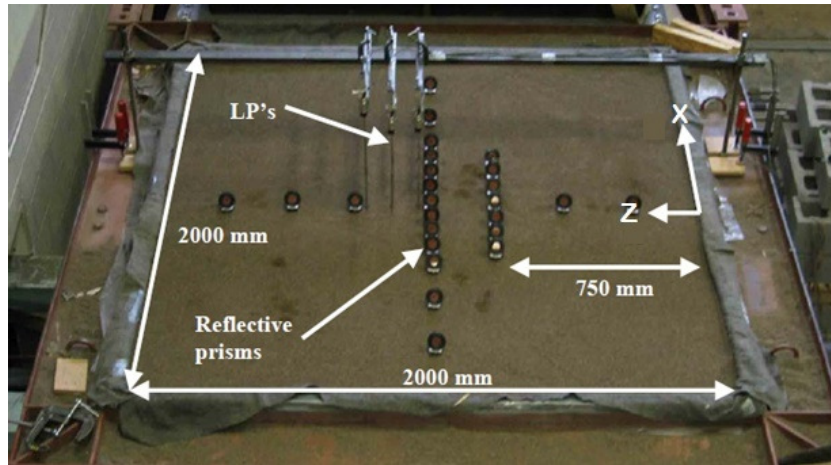


Figure 3. Surveying prisms placed on the surface to measure ground deformations (Lapos, 2004)

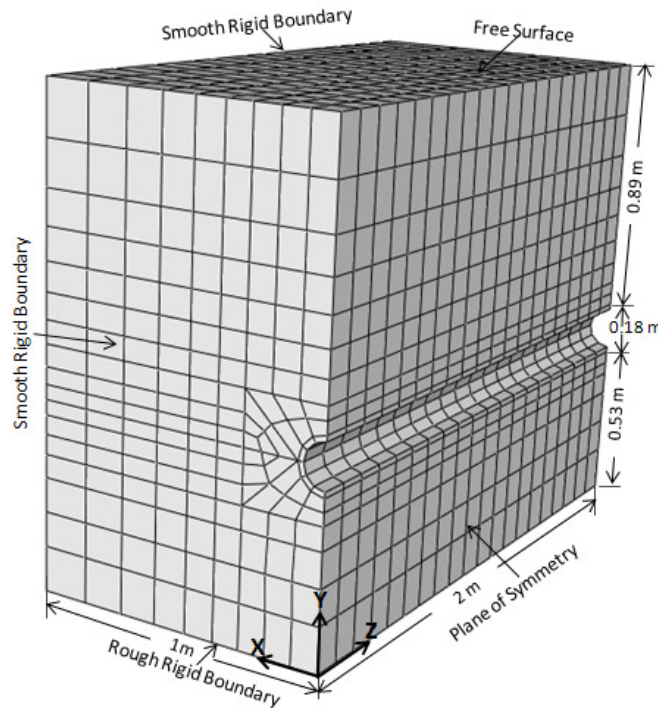


Figure 4. The geometry, boundary conditions, and mesh used for 3D analysis of the pipe bursting experiment.

## 2. DETAILS OF THE FINITE ELEMENT MODEL

Finite element calculations were performed using ABAQUS 6.7 (Hibbit et al. 2007) since this algorithm includes master-slave interface models to characterize the large body-to-body sliding movements associated with pipe bursting. Mesh dimensions were selected to match those of the pipe bursting experiments of Lapos et al. (2004) as shown in Figure 4. The mesh boundary was then extended two times in the lateral direction for overlying pipeline analysis in order to eliminate boundary effect (Figures 5 and 6). As the test cell was symmetric with respect to the vertical plane through the axis of the clay pipe, only half of the cell was meshed to significantly reduce the

computational cost. The inside diameter (ID) of the old clay pipe was 146 mm and the thickness was 19 mm. The largest diameter of the burst head was 202 mm and the length of that cylindrical section of the burst head was 165 mm. The ID of the replacement pipe was 145 mm and wall thickness was 10 mm. The PVC pipe had ID of 115 mm and thickness of 7 mm. The dimensions of the CI pipe were initially set to be the same as the PVC pipe for comparison purposes. However, the thickness of the CI pipe was then changed to study the effect of relative thickness ( $D/t$ ). Two extreme cases ( $D/t = 11.2$  and  $D/t = 31.5$ ) reported for water mains in Toronto (Seica et al, 2002) were considered for comparison. Separate analyses were conducted for overlying pipe oriented transverse to and parallel to the direction of bursting, Figures 5 and 6 respectively.

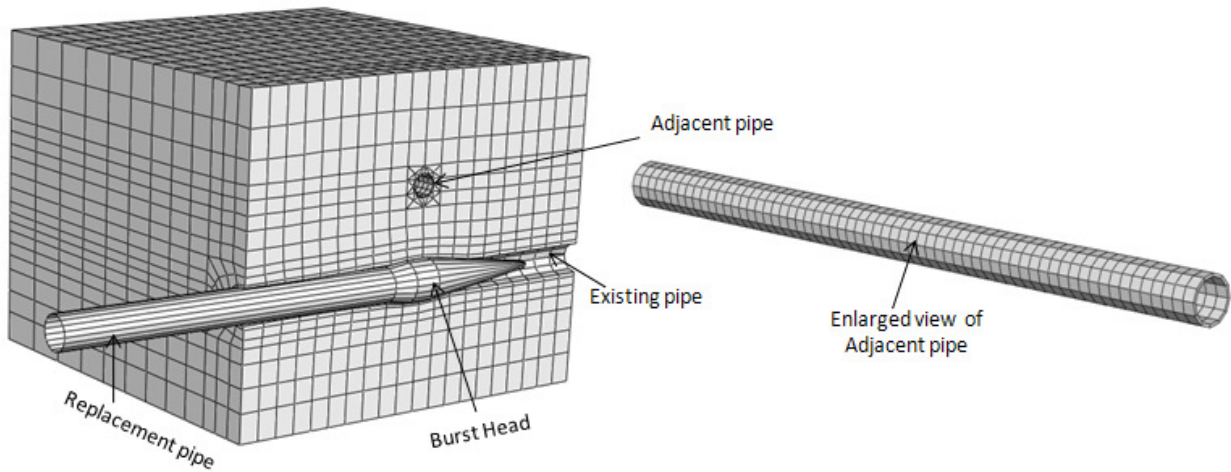


Figure 5. The finite element mesh for the analysis of an overlying pipe oriented transverse to the bursting direction

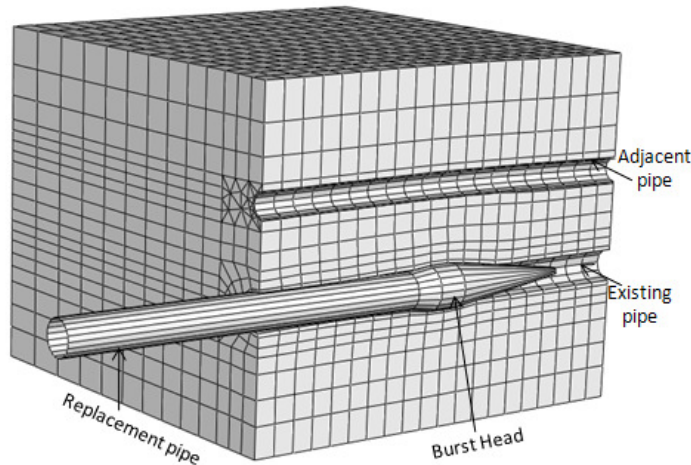


Figure 6. The finite element mesh for the analysis of an overlying pipe running parallel to the bursting direction

The soil was modeled as an elastic perfectly plastic continuum, based on the Mohr-Coulomb model with a friction angle of  $44^\circ$ . A small cohesion intercept of 1kPa was applied to increase numerical stability. Since ground movements caused by pipe bursting in dense coarse-grained soils are dominated by dilation, a non-associated flow rule was employed. Triaxial tests were undertaken on the test sand, providing initial dilation angle of  $16^\circ$ , and gradual decrease in dilation to  $0^\circ$  at larger shear strains, and the test measurements and approximations associated with this dilation model are shown in Figure 7. Elastic modulus was modeled using the stress-dependent modulus model of Janbu (1963), with Janbu parameters  $K$  and  $n$  of 340 and 0.81 respectively (Lapos and Moore, 2002). The vitrified clay pipe being replaced was modeled as having high initial strength, which was subsequently converted to

the same material as the soil after breakage. The burst head was modeled as a conical shaped analytical rigid body, followed by a short cylinder, a taper, then the external cylindrical surface representing the new pipe being installed. The adjacent PVC and cast iron pipes were modeled as linear elastic materials with elastic moduli of 3000 MPa and 96000 MPa for the polymer and metal materials, respectively (Balkaya and Moore, 2009; Seica et al, 2002).

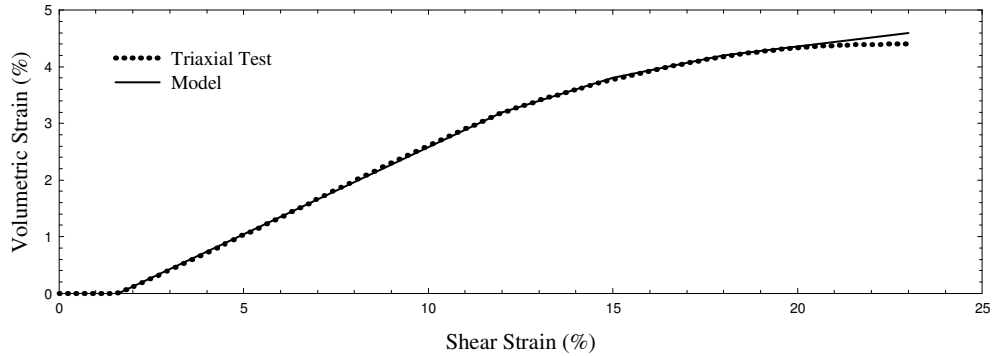


Figure 7. Volumetric strain versus shear strain in a triaxial test measurement and numerical approximations

The boundary conditions of the model are shown in Figure 4. A rough rigid boundary condition was applied at the base of the mesh. The two sides and back of the mesh were modeled as smooth rigid boundaries. A symmetric boundary was applied on the plane of symmetry (the plane cutting vertically through the clay pipe axis). The top surface was left free. The motion of the burst head was controlled by the 'Reference Point' of the analytical rigid body. The burst head was allowed to move in the vertical direction so that it is free to move upward towards the unrestrained ground surface. The high strength material of the old pipe acts as a stiff boundary between the soil and the pipe cavity before the pipe is broken, and after breaking the outside surface of the replacement pipe interacts with the soil (the inner surface of the old pipe is then modeled as the inner surface of the soil boundary).

The finite element meshes used are shown in Figures 5 and 6. The existing pipe, the surrounding soil and the adjacent pipes were meshed using 8 noded elements. Six noded elements were applied to the soil surrounding the overlying pressure pipe. The rest of the mesh was composed of 8 noded hexahedral (brick) elements. 'Penalty' type 'surface to surface' interaction was applied between the old clay pipe and the burst head. 'Node to surface' interaction was employed at the soil - pipe interfaces.

### 3. RESULTS

The vertical deformations of the surface along a line parallel to the x-axis located at the middle position of the model are shown in Figure 8. The estimates of peak vertical deformation are within 10% of values measured during the laboratory test. The incremental strain profiles (longitudinal, radial and circumferential) calculated for the overlying pressure pipelines during the complete progression of the burst head are obtained from these calculations. Figure 9 shows such strain profiles for the transverse PVC pipeline. The figure reveals that the largest strains are in the longitudinal direction of the adjacent pipeline. The radial and circumferential strains are the result of Poisson's effect. The figure illustrates the strain profiles of two points on the PVC pipe - one on the crown another on the invert located directly above the clay pipe being replaced. The longitudinal strains are tensile at the crown and compressive at the invert of the pipe for this location. The radial and circumferential strains are of opposite sign, and these two strain components are almost equal at the crown of the pipe. However, radial strains exceed the circumferential strains at the invert of the pipe. All the strains (longitudinal, radial and circumferential) gradually increase as the burst head approaches, and then gradually decrease as the burst head moves away. The peak strains (about 0.2%) occur when the largest diameter of the burst head is directly below the pressure pipe.

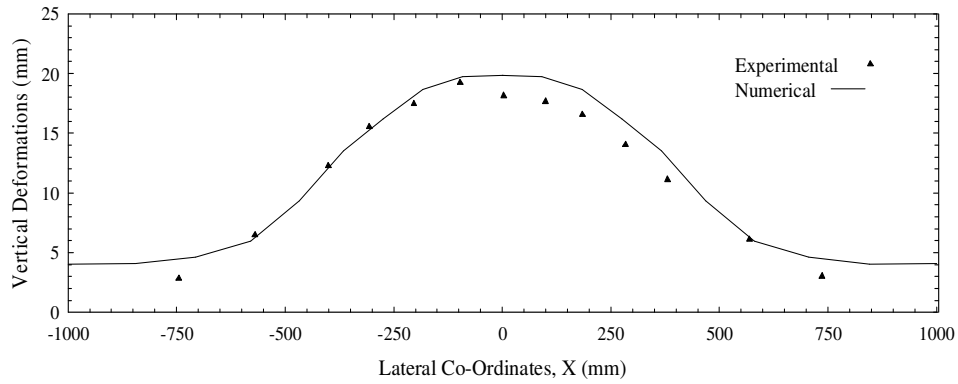


Figure 8. Comparison between vertical deformations measured and calculated

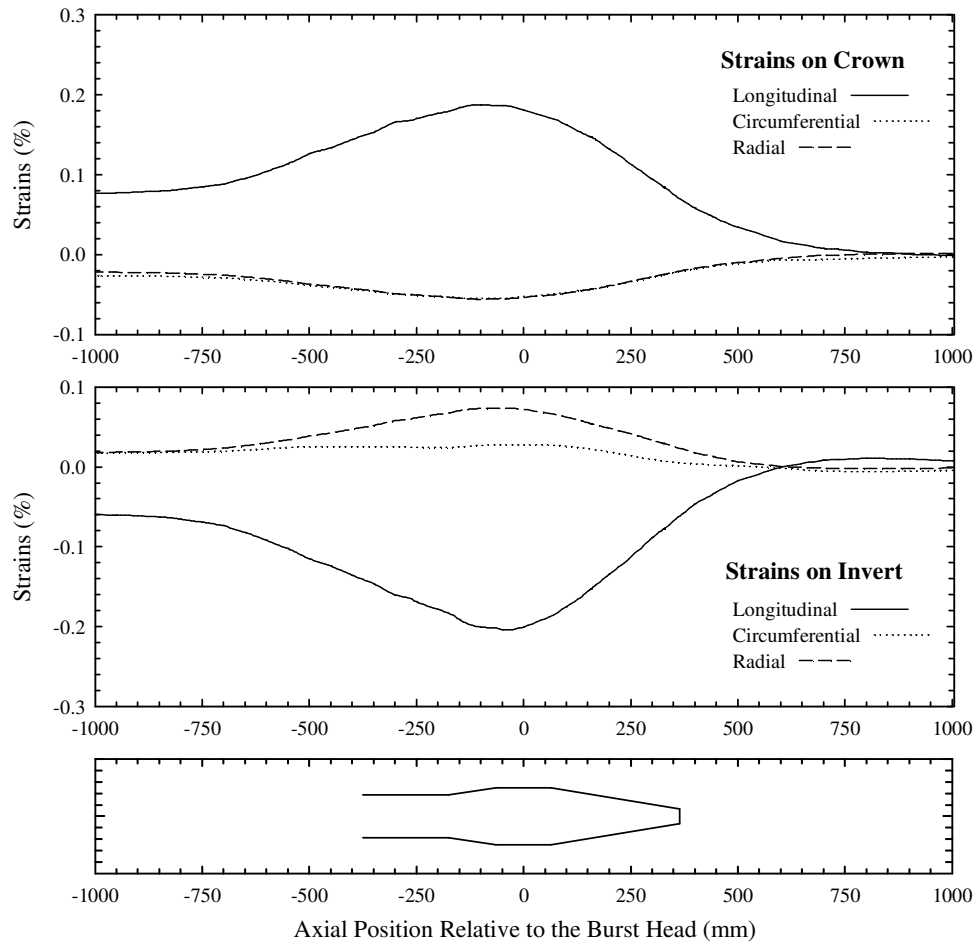


Figure 9. Strain profiles at the crown and invert of the transverse pressure pipeline at a position directly above the pipe being replaced by bursting; strains plotted as a function of the position of the burst head.

Figure 10 shows the longitudinal strain distributions along the crown and invert of the overlying pressure pipe when burst head is directly below it. The maximum longitudinal strain in the pressure pipe occurs directly above the pipe being replaced. At the crown, strain is tensile, and gradually decreases and becomes compressive at a distance approximately 600 mm from the centerline of the pipe being replaced. The longitudinal strain distribution at the invert of the pressure pipe is essentially equal and opposite to the values along the crown, although the magnitude of the strains is slightly higher.

Figure 11 illustrates the stress distribution along the transverse PVC pipe when the burst head is located directly below the PVC pipe. The crown of the pipe experiences peak tensile stress at a point directly above the pipe being replaced, and it experiences peak compressive stress at approximately 1000 mm from that position. The stress distribution along the invert is opposite to that along the crown. The peak stress (both tensile and compressive) is around 6.5 MPa.

The vertical deformations for the PVC pipe are shown in Figure 12. This indicates that the vertical deformation of the invert is 14 mm, which is higher than the crown movement of 10 mm, likely because the invert is closer to the bursting operations below. This means the vertical diameter of the PVC pipe decreased by 3.7%. Again, maximum vertical deformations occur when the burst head is directly below.

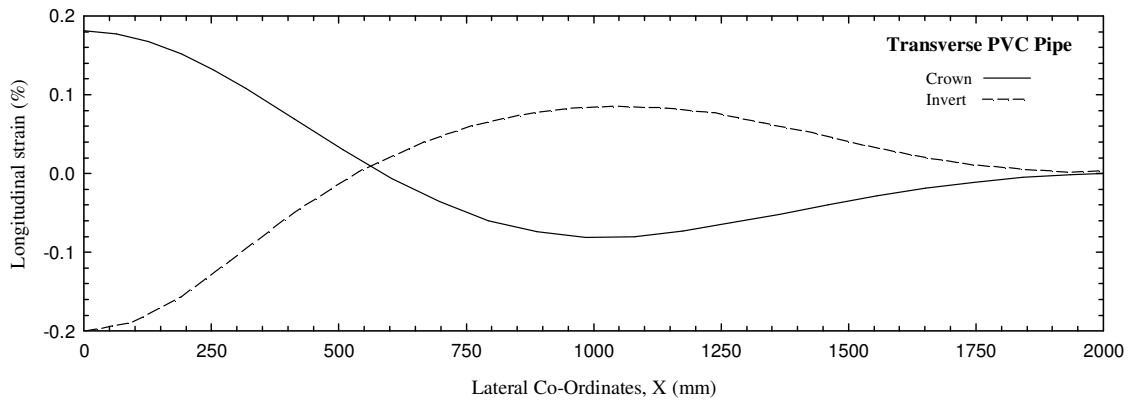


Figure 10. The distribution of longitudinal strain along the crown and invert of the overlying PVC pressure pipe running transverse to the pipe being replaced; values are shown for burst head located directly below

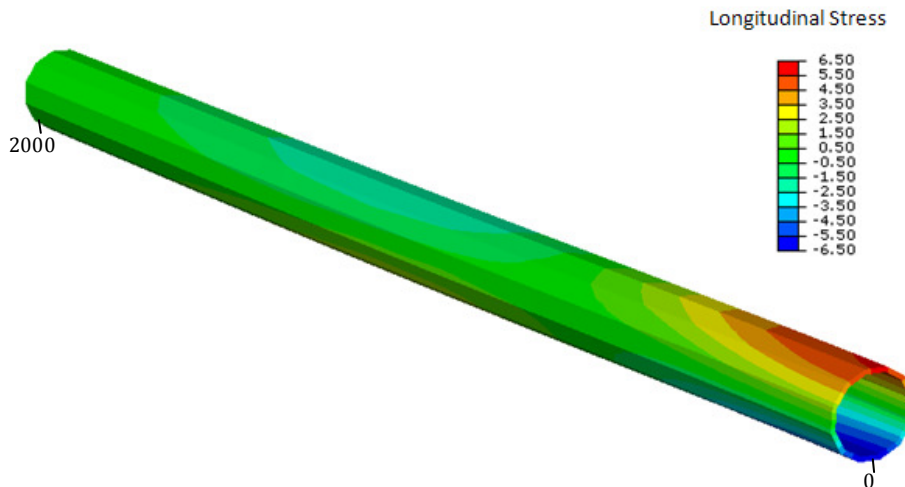


Figure 11. The contours of longitudinal stress of the overlying PVC pressure pipe running transverse to the pipe being replaced; values are shown for burst head located directly below

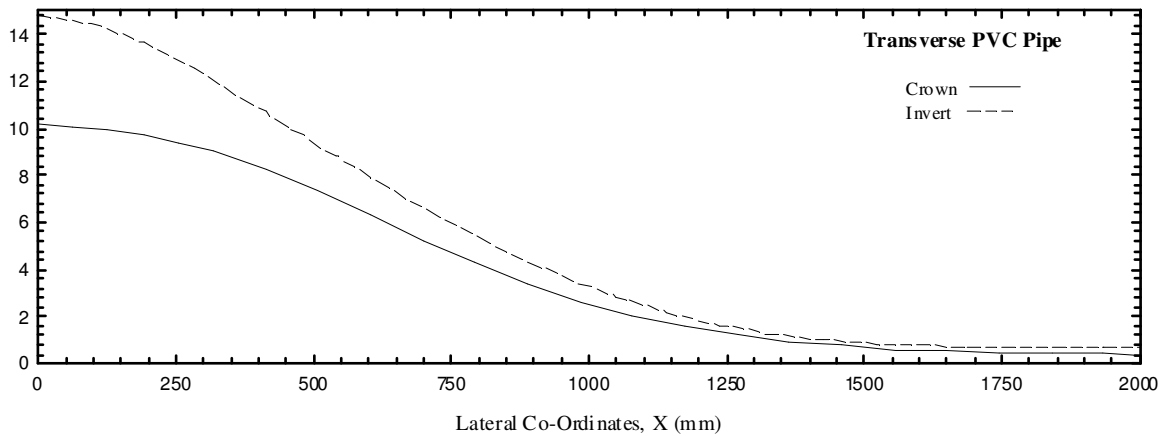


Figure 12. The vertical deformations along the crown and invert of the overlying PVC pressure pipe running transverse to the pipe being replaced; values are shown for burst head located directly below

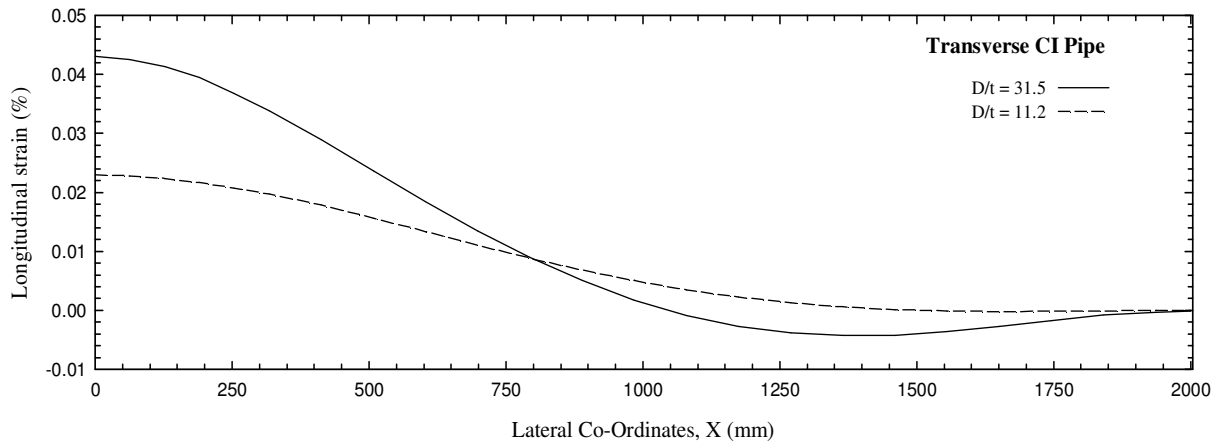


Figure 13. The distribution of longitudinal strain along the crown of the overlying CI pipes (with different relative thickness) running transverse to the pipe being replaced; values are shown for burst head located directly below

The patterns of strain, stress and deformation for a cast iron (CI) pipe at the same location are similar to the PVC pipe, but with different magnitude. However, that magnitude depends on the relative thickness of the pipe. Clearly the thin cast iron pipe ( $D/t = 31.5$ ) is more flexible than the thick ( $D/t = 11.2$ ) structure, and experiences more strain than the thick pipe (Figure 13). The peak incremental longitudinal strain in the simulated CI pipe is about 0.043%, which is below the failure strain (minimum 0.07%) of cast iron water pipes reported by Seica et al. (2002). However, this is incremental strain resulting from ground movements associated with pipe bursting, and does not include the effects of thermal changes and internal pressure. Depending on the level of safety used in the original pipe design, strain of this magnitude may be sufficient to cause fracture.

Further analysis was conducted by simulating PVC and CI pipes of the same dimensions but oriented parallel to the existing pipe being replaced (the configuration shown in Figure 6). Figure 14 illustrates the longitudinal strains along the PVC pipe for burst head located at the middle position. These calculations indicate that the pressure pipe overhead experiences peak longitudinal strains at the position directly above the burst head. The peak longitudinal strain calculated for the PVC pipe is about 0.2%, the maximum uplift movement is about 23 mm (Figure 15), and the maximum change in vertical pipe diameter is over 5%. Figure 16 provides strain distributions for the parallel CI pipe, which experiences less strain than seen earlier in Figure 13 for the transverse CI pipe. The peak longitudinal strain calculated for the thin CI pipe is 0.023%, which is significantly higher than that calculated for the thicker cast

iron pipe. This is because the thicker cast iron pipe has much higher longitudinal bending stiffness, which suppresses uplift and the peak curvature that results.

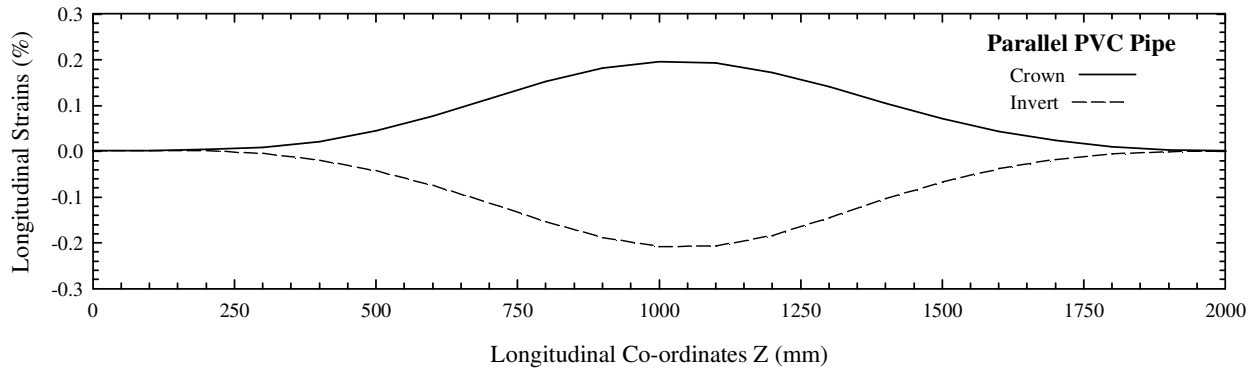


Figure 14. The distribution of longitudinal strains along the crown and invert of the overlying parallel PVC pipe when the axial position of the burst head is at Z of 1000 mm

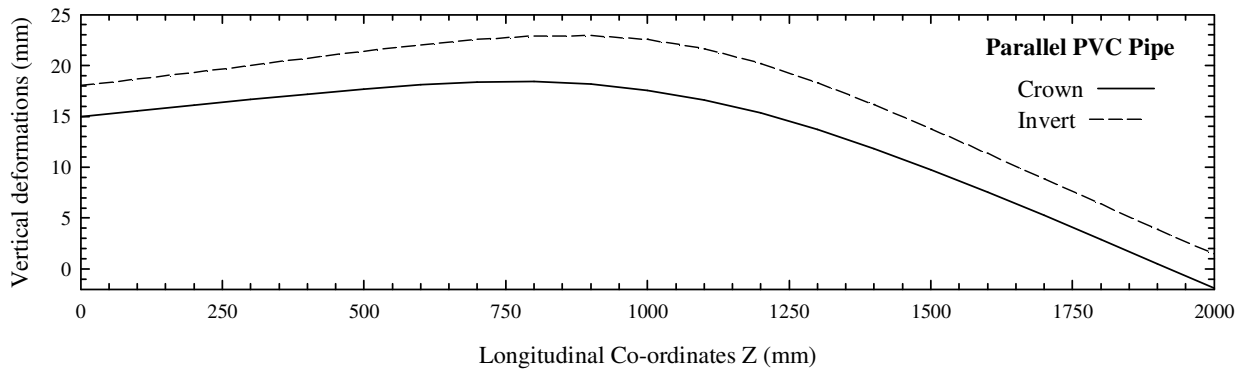


Figure 15. The distribution of vertical deformations along the crown and invert of the overlying parallel PVC pipe when the axial position of the burst head is at Z of 1000 mm

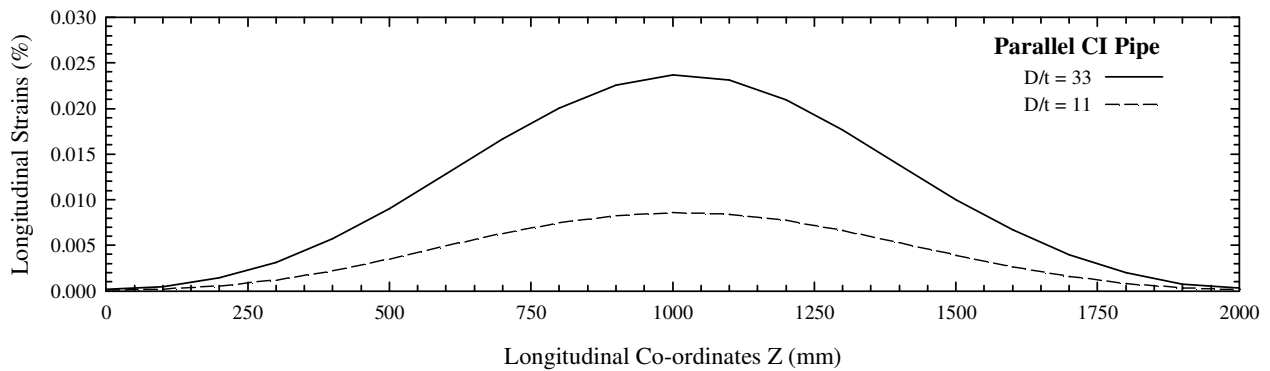


Figure 16. The distribution of longitudinal strains along the crown and invert of the overlying parallel CI pipe (with different relative thickness) when the axial position of the burst head is at Z of 1000 mm

#### 4. CONCLUSIONS

The strains, stresses and deformations in adjacent pipelines have been calculated using three dimensional finite element analyses. The overlying pressure pipes oriented both transverse and parallel to the pipe being replaced developed maximum strains in the longitudinal direction, and these occurred when the burst head was directly beneath the overlying pipe. The peak longitudinal strains in the PVC and CI water pipes were about 0.2% and 0.04% respectively. This additional strain in cast iron pipe may be sufficient to cause fracture. The maximum vertical deformation of the PVC pipe was about 23 mm, and this pipe experienced more than 5% decrease in vertical pipe diameter since the vertical deformation of the invert of the PVC pipe was significantly higher than the crown.

The three dimensional modeling techniques that have been developed have been used to explore the key mechanisms of behaviour, and could be used to provide estimates for critical pipe infrastructure. These tools are currently being used to develop simplified design methods for estimation of pipe bursting impacts on adjacent pipelines.

#### 5. REFERENCES

- Atalah, A., Sterling, R., Hadala, P., and Akl, F. (1997). The Effect of Pipe Bursting on Nearby Utilities, Pavement, and Structures. Technical Report, Trenchless Technology Center, Louisiana Tech University
- Balkaya, M., Moore, I. D. (2009). Analysis of a Gasketed Polyvinyl Chloride Pipe Joint, Transportation Research Record, No. 2131, pp 113-122.
- Brachman, R. W. I., Moore, I. D., and Rowe, R. K. (2001). The Performance of a Laboratory Facility for Evaluating the Structural Response of Small-diameter Buried Pipes. Canadian Geotechnical Journal, 38(2), 260-275.
- Hibbitt, H. D., Karlsson, B. I., and Sorensen, E. P. (2007). ABAQUS User Manual, Version 6.7, ABAQUS Corporation, USA
- Janbu, N. (1963). Soil Compressibility as Determined by Oedometer and Triaxial Test, Proceedings of the European Conference on Soil Mechanics and Foundation Engineering, Vol. 1, pp 19-25, Weisbaden.
- Lapos, B. (2004). Laboratory Study of Static Pipe Bursting, MSc Thesis, Queens University, Kingston, Ontario, Canada
- Lapos, B., and Moore, I. D. (2002). Evaluation of the Strength and Deformation Parameters of Olimag Synthetic Olivine, Proceedings of the 55<sup>th</sup> Canadian Geotechnical and 3<sup>rd</sup> Joint IAH-CNC and CGS Groundwater Specialty Conferences, Niagara Falls, Ontario, October 20-23, 2002
- Lapos, B., Brachman, R.W.I., Moore, I.D., (2004). "Laboratory Measurements of Pulling Force and Ground Movement During a Pipe Bursting Test", NASTT, No-Dig March 22-24, 2004, New Orleans, Louisiana.
- Rogers, C. D. F., and Chapman, D. N. (1995). Ground movements caused by trenchless pipe installation techniques. Transportation Research Record, (1514), 37-48.
- Seica, M. V., Packer, J. A., Grabinsky, M.W.F. and Adams B. J. (2002). Evaluation of the Properties of Toronto Water Mains and Surrounding Soil, Canadian Journal of Civil Engineering, Vol. 29, pp 222-237.